Appl. Phys. A (2015) 121:779–788
DOI 10.1007/s00339-015-9366-y

Applied Physics A
Materials Science & Processing

INVITED PAPER

Blanching of paint and varnish layers in easel paintings: contribution to the understanding of the alteration

Anaïs Genty-Vincent[1,2,3] · Myriam Eveno[1] · Witold Nowik[1] · Gilles Bastian[1] · Elisabeth Ravaud[1] · Isabelle Cabillic[1] · Jacques Uziel[2] · Nadège Lubin-Germain[2] · Michel Menu[1,4]

Received: 7 April 2015 / Accepted: 14 July 2015 / Published online: 28 July 2015

Abstract The blanching of easel paintings can affect the varnish layer and also the paint layer with a blurring effect. The understanding of the physicochemical and optical phenomena involved in the whitening process remains an important challenge for the painting conservation. A set of ca. 50 microsamples from French, Flemish, and Italian blanched oil paintings, from sixteenth to nineteenth century, have been collected for in deep investigations. In parallel, the reproduction of the alteration was achieved by preparing some paint layers according to historical treatises and altering them in a climatic chamber in a humid environment or directly by immersing in ultrapure water. The observation of raw samples with a field-emission gun scanning electron microscope revealed for the first time that the altered layers have an unexpected highly porous structure with a pore size ranging from ca. 40 nm to 2 μm. The formation mechanism of these pores should mostly be physical as the supplementary analyses (Fourier transform infrared spectroscopy, gas chromatography–mass spectrometry) do not reveal any noticeable molecular modification. Considering the tiny size of the pores, the alteration can be explained by the Rayleigh or Mie light scattering.

✉ Anaïs Genty-Vincent
anais.genty@culture.gouv.fr

[1] Centre de Recherche et Restauration des Musées de France (C2RMF), Palais du Louvre - Porte des Lions, 14 Quai François Mitterrand, 75001 Paris, France

[2] Laboratoire de Chimie Biologique (LCB), EA 4505, Université de Cergy-Pontoise, 5 Mail Gay-Lussac, Neuville-sur-Oise, 95031 Cergy-Pontoise Cedex, France

[3] Fondation des sciences du Patrimoine, Patrima, 33, boulevard du Port, 95011 Cergy-Pontoise Cedex, France

[4] Chimie ParisTech-CNRS, Institut de Recherche Chimie Paris, UMR8247, PSL Research University, 75005 Paris, France

1 Introduction

Blanching of easel paintings is a recurring alteration that can affect the varnish layer and also the paint layer, strongly altering the visual aspect of the paintings. Treatments currently used are not suitably efficient. The understanding of such an alteration therefore remains an important challenge for the painting conservation.

This alteration is known to appear on paintings kept in a humid environment or to be the result of aqueous conservation treatments with a possible heat source, such as (re)-lining or fixation of loose paint [1–4]. Blanching, however, is not systematic. The majority of the paintings that have been relined do not present any sign of blanching. Besides, altered and unaltered areas can coexist within a same color range. Considering the complexity of this phenomenon and despite several studies dated mainly from the 1980 and 1990s, its nature has never been clearly identified [1, 2, 5–7]. Several hypotheses have been proposed: a possible modification of the binder refractive index [2, 3, 7] or an apparition of microstructures (microvoids, microcracks, microcrystallization, microprecipitation, microemulsion,…) resulting in multiple light reflection in the layer [4, 6, 8, 9]. Free fatty acid migration has also been considered as a probable cause [10]. More recent studies [11, 12] have concluded that blanching could also be the consequence of a lead soap accumulation on the paint layer surface.

The aim of the present work was to better understand the physicochemical and optical phenomena involved in the

whitening process. A set of ca. 50 paint microsamples collected from the sixteenth to the nineteenth century French, Flemish, and Italian blanched oil paintings, as well as mock-up samples, have been studied. This work is based on a multiscale approach. Structural modifications have been highlighted at a macroscale by 3D digital microscopy and at a micro-/nanoscale by field-emission gun scanning electron microscopy (FEG-SEM). Investigations at the molecular scale have been performed by Fourier transform infrared spectroscopy (FTIR) and gas chromatography–mass spectrometry (GC–MS).

2 Experimental

2.1 Samples

A set of ca. 40 paint microsamples have been collected from 12 French, Flemish, and Italian blanched oil paintings, ranging from the sixteenth to the eighteenth centuries. Another set of ca. 10 microsamples have been taken from two paintings, one dating from the second part of the seventeenth century and the other dating from the nineteenth century in order to study the blanching of varnish layers (Table 1).

In parallel, a series of mock-ups were made according to historical treatises [13–17] and our first results obtained from the analysis of ancient paintings. The effects of three parameters were tested: the binder preparation, the nature of the pigments, and the presence of an extender (*i.e.* , chalk–calcium carbonate). Two different recipes were used to prepare a lead medium. The first one is inspired from the *Formula for the second lead medium, probable technique of Leonardo da Vinci*, given by Maroger [13] and from a recipe described in 1633 in Folio 28 of Turquet de Mayerne's treatise [14]. This recipe has already been reproduced by Cotte et al. [15, 16]. The second one is based on the recipe of black oil given by Yvel [17] for the oil/litharge ratio and on Maroger [13], who recommends the addition of water to get a lighter medium with a better consistency.

Both binders were made from walnut oil (HMB-BDA, France), water, and PbO (Merck-Eurolab-Prolabo, France) in the mass proportions 4-4-1 (recipe 1) and 10-10-1 (recipe 2). PbO was first ground with oil. This mix was heated for 40 min at 60 °C. After adding water, it was heated at 100 °C for 180 min. Binders were then ground with pigments with or without chalk and applied on microscope glass slides. The relative quantities of binder, pigments, and chalk used for the preparation of the painting mock-ups are given in Fig. 1. As blanching is localized principally on green, brown, blue, and dark areas [1, 2, 9, 18], the following four pigments have been used: raw umber (Kremer, 40612, Germany), green earth (Sennelier, 213, France), black ivory (Kremer, 12000, Germany), and azurite (Kremer, 10200, Germany).

Two slides were prepared for each composition. After 2 months of drying, one slide was put in a climatic chamber (Suntest XXL+, Atlas) with alternately humid and dry conditions. The xenon arc lamp used with a window glass filter was set at 50 W/m^2 in the 300–400 nm range. The following cycle has been done three times to simulate a relining (aqueous conservation treatments with heat source). Step 1: 50 °C, 40 % RH (relative humidity); Step 2: 40 °C, 60 % RH; Step 3: 40 °C, 80 % RH; Step 4: 40 °C, 60 % RH; 30 h per step. The obtained mock-ups are presented in Fig. 1.

To simulate water damage, the reproduction of the alteration for varnish was achieved by immersing varnish layers applied on microscope slides in ultrapure water from 0 to 31 days. Natural resins (mastic and dammar) as well as synthetic resins (Paraloid B72, Laropal A81, Regalrez 1094, MS2A) were tested. More information about these resins can be found in [19, 20]. The evolution of alteration was followed visually for 31 days, and samples were taken and observed by FEG-SEM after 1.5, 10, 15, and 31 days.

2.2 Methods

2.2.1 3D digital video microscopy and optical microscopy

Samples were first observed with a 3D digital video microscope, Hirox KH 8700, coupled with a revolver zoom lens MXG-2500REZ (magnification from ×35 up to ×2500). The 3D images allow us to determine the topography but also to distinguish precisely, at high magnification, the altered and unaltered areas within a sample. The samples have also been observed under UV-light illumination to highlight the presence of varnish with an optical microscope (Nikon Labophot-2) coupled with a Nikon DS-Ri1 camera.

2.2.2 Field-emission gun scanning electron microscopy (FEG-SEM)

Field-emission gun scanning electron microscopy was performed on a JSM-7800F with the PC-SEM version 5.1.0.1 software (JEOL). Samples were observed without any preparation and without coating. Secondary electron (SE) images were collected at 1 kV with a probe current of ca. 18–20 pA and a working distance of ca. 6–7 mm.

2.2.3 Fourier transform infrared spectroscopy (FTIR)

Mock-up samples were analyzed by Fourier transform infrared spectroscopy in a diamond cell. The analyses were

Table 1 Complete references of the 13 studied paintings including the sampled layers and their colors

Painter	Title	Date	Museum	Inventory number	Size (mm^2)	Altered layer	Color
D'Oggiono, Marco (pupil of Leonardo da Vinci) (ca. 1467–1524)	La cène	1506	Musée national de la renaissance, Ecouen	INV781	2600 × 5490	Paint and varnish	Publish, orange, brown, dark
Anonymous	Descente de croix	1600–1650	Musée des Beaux-Arts, Carcassonne	890.9.145	930 × 1190	Paint	Brown, dark, blue
Sandrart, Joachim 1 von (1606–1688)	Sainte famille dans un paysage	1606–1688	Musée des Beaux-Arts, Rennes	801.1.27	1292 × 1365	Paint	Green
Van der Meulen, Adams Frans (1632–1690)	Siège de Courtrai	Ca. 1667	Musée National du chateau de Versailles et du Trianon	MV5846/INV 1477/LP 2836	2300 × 3260	Paint	Green
Van der Bent, Johannes (ca. 1650–1690)	Paysages, figures et animaux	1650–1690	Musée des Beaux-Arts, Rennes	794.1.3	950 × 1250	Paint	Light and dark brown, dark
Anonymous	L'Aurore	1650–1700	Musée du Louvre, Paris	INV8690	1880 (diameter)	Paint	Flesh color, orange, light and dark brown, green purplish, black
Van Schrieck, Otto Marseus (1619–1678)	Chardons, écureuils, reptiles et insectes	Ca. 1660–1678	Musée des Beaux-Arts, Quimper	873.1.367	1355 × 1020	Paint	Dark blue
Cotelle, Jean (the younger) (1645–1708)	Vue de la fontaine de l'Encelade avec Jupiter foudroyant	1650–1700	Musée National du château de Versailles et du Trianon	MV735	2015 × 1375	Paint and varnish	Green
Cotelle, Jean (the younger) (1642–1708)	Vue des cinquante-deux jets de Trianon avec Mars et Vénus devant Apollon et Vulcain qui va les faire prisonnier avec un filet	1688	Musée National du château de Versailles et du Trianon	MV777	2030 × 2290	Paint	Green
Desportes, Alexandre François (1661–1743)	Chiens et gibier mort	1726	Musée de la chasse et de la nature, Paris,	INV3934	1100 × 1360	Paint	Green
Nattier, Jean Marc (workshop of) (1685–1766)	Portrait de Louise-Marie de France, dite Madame Louise	Ca. 1750	Musée National du château de Versailles et du Trianon	MV 4442	1345 × 1046	Paint	Green, brown
Chardin, Jean Baptiste Siméon (1699–1779)	Les Attributs des arts	1765	Musée du Louvre, Paris	INV3199	910 × 1450	Paint	Dark brown
Crignier, Louis (1790–1824)	Jeanne d'arc en prison	1824	Musée des Beaux-Arts, Amiens	MP récol.90.2.83	1164 × 885	Varnish	–

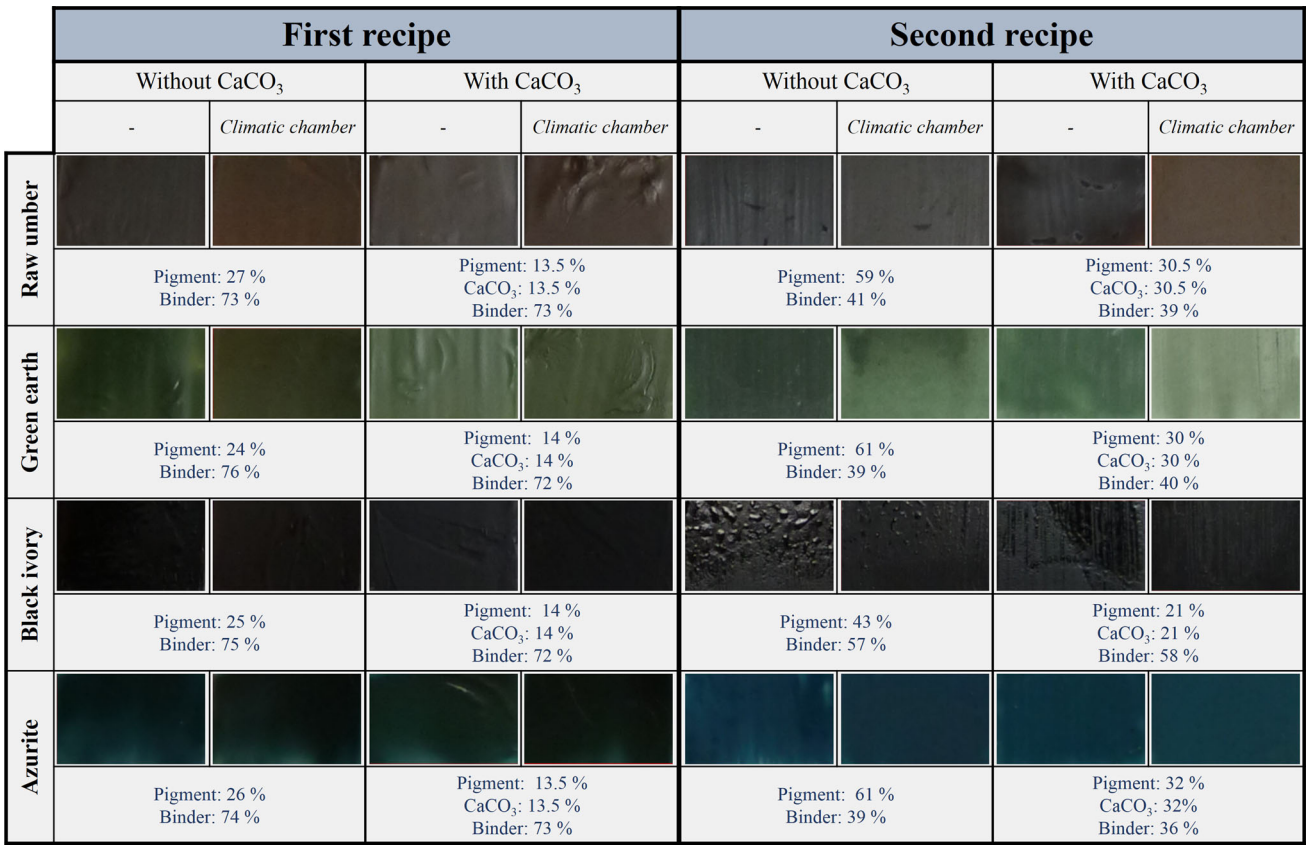

Fig. 1 Photograph in visible light (details) of the mock-ups prepared from two recipes with four pigments (*raw umber*, *green earth*, *ivory black*, and *azurite*) with or without calcium carbonate. Half of the microscope slides were placed in a climatic chamber. The mock-ups A and B present an important alteration

performed with a PerkinElmer FTIR-Spectrum 2000 using a deuterated triglycine sulfate (DTGS) detector and a cesium iodide (CsI) beam splitter. The spectra were collected in the 4000–400 cm^{-1} range with a spectral resolution of 4 cm^{-1} (64 scans).

2.2.4 Gas chromatography–mass spectrometry (GC–MS)

Mock-up samples (paint or varnish layers) as well as samples from the painting of Louis Crignier (1790–1824), *Jeanne d'arc en prison* (varnish), were analyzed by gas chromatograpy–mass spectrometry after appropriated derivatization. GC–MS system equipped with a quadripole mass spectrometer detector (Shimadzu GCMS-QP2010) was employed for analyses. Chromatographic separation was performed after splitless injection on CP-Sil 8CB 30 m capillary column of 0.25 mm internal diameter with 0.25 µm film thickness.

The injector temperature was set at 310 °C, transfer line 320 °C, and temperature programming started from 80 °C isothermal for 2 min, then heating rate 7 °C/min to 150 °C, then another heating rate of 4 °C/min up to 340 °C, and finished by 5 min isothermal segment. Helium was the carrier gas working in linear velocity regime at 36.3 cm/s. Mass spectrometry relied on ionization by electron impact of 70 eV in the source maintained at 200 °C. The mass range was 50–950 m/z.

Varnish samples of about 50–200 µg were silylated with 50 µL BSTFA + 1 % TMCS (Supelco, Bellefonte, PA, USA) at 75 °C for 30 min and then evaporated with N_2. The residue was solubilized in CH_2Cl_2 in proportion of 10µL for 100 µg of solid sample. In parallel, the same samples were methylated with Meth-Prep II (Grace, Deerfield, IL, USA) and toluene (1:1, v/v) at 75 °C for 30 min using the same sample quantities and reaction mixture in the same proportion as for CH_2Cl_2 in former derivatization procedure. Paint layer samples were only methylated in proportion of 150 µL of reagents for ca. 100 µg of solid sample. An aliquot of 1 µL of solutions containing derivatized compounds was injected to the GC–MS system.

3 Results and discussion

3.1 Blanching of varnish layers

This part of the study is based on samples from two paintings: Louis Crignier (1790–1824), *Jeanne d'Arc en prison* and Jean Cotelle (1642–1708), *Vue de la fontaine de l'Encelade avec Jupiter foudroyant* (Table 1). The results obtained on both paintings are comparable, and only the analysis performed on samples from the first one will be presented. The blanching of the varnish layer on this painting originates from a water damage and is principally localized on the right side and bottom of the painting due to water flow because of water retention in the frame (Fig. 2a). The visual appearance is strongly altered in these areas, and the paint composition is not visible through the blanched varnish.

The examination of the sample, positioned on its edge, with a 3D digital videomicroscope revealed the following stratigraphy (Fig. 2b): a white ground layer (1), a dark brown paint layer (2), and three layers at the top (3–5) which are varnish layers according to the observation done under UV-light illumination (Fig. 2c). Whereas layer 5 is oxidized but still translucent, layer 3 has become white and opaque.

Analyses have been performed by FTIR spectroscopy and by GC–MS to determine the nature of the varnish and if the whitening is linked to a chemical transformation. The varnish has been identified by FTIR spectroscopy as a natural triterpenic resin thanks to the presence of the following characteristic peaks: ca. 3410 cm^{-1} (−OH stretching band); 2947–2953 and 2877 cm^{-1} (methylic ($-CH_3$ and $-CH_2$) stretching band); 1711 cm^{-1} (C=O stretching band); 1456 and 1385 cm^{-1} (C–H bending band); and 1259 cm^{-1} (C–O stretching band) (Fig. 3a). The methylated samples analyzed by GC–MS reveal the presence of derivatives of oleanoate skeleton characterized by abundant ions 189 and 203 m/z (Fig. 3b) [21]. The presence of these compounds as well as the comparison with standard mastic sample allows identifying this resin as mastic, although the precise compound identification was not done. However, from this results, the most important information is that no significant differences have been brought to light between altered and unaltered samples (Fig. 3). The same conclusion can be drawn from the analyses of mock-up samples.

Altered and unaltered samples have been then studied with a field-emission gun scanning electron microscope (FEG-SEM). An innovative and successful approach requiring no sample preparation has been developed to

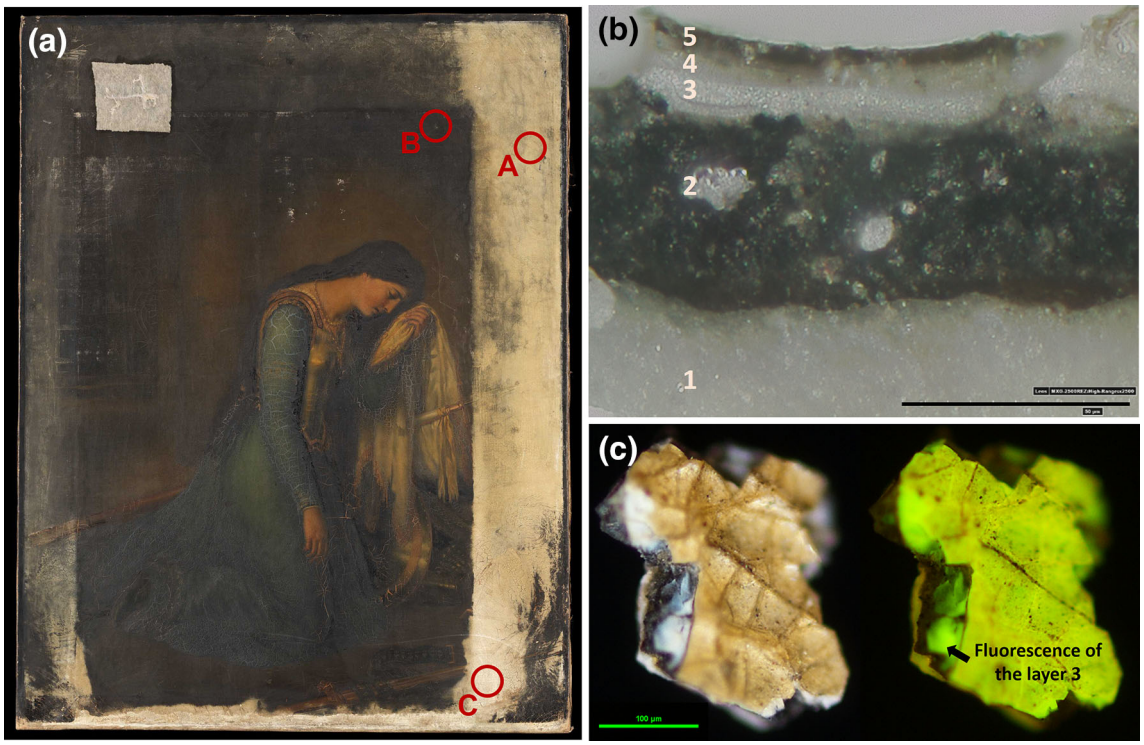

Fig. 2 **a** Photograph in visible light, Louis Crignier, Jeanne d'Arc en prison, 1164 × 885 mm^2 ©C2RMF/A. Maigret; Parts on the right and on the bottom are altered. *A* altered sample; *B* unaltered sample; *C* much altered sample; **b** Edge of the sample A by 3D digital videomicroscope. *1* white ground; *2* brown layer; *3–5* varnish layers. *Scale bar* 50 µm; **c** Sample A under visible (*left*) and UV (*right*) light with an optical microscope. *Scale bar* 100 µm

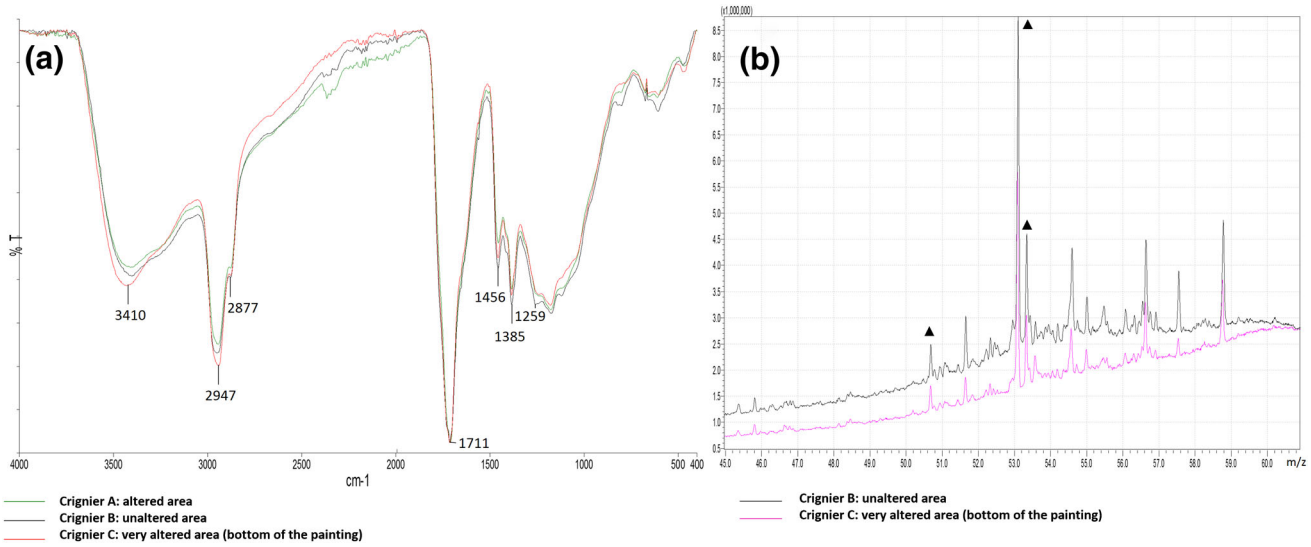

Fig. 3 Varnish samples from Louis Crignier, Jeanne d'Arc en prison. **a** FTIR spectrum of an unaltered sample B (*black*), an altered sample A (*green*), and a much altered sample C (*red*); **b** GC–MS chromatogram of an unaltered sample B (*black*) and a much altered sample C (*pink*) with several peaks of oleanoate analogues (*triangle*)

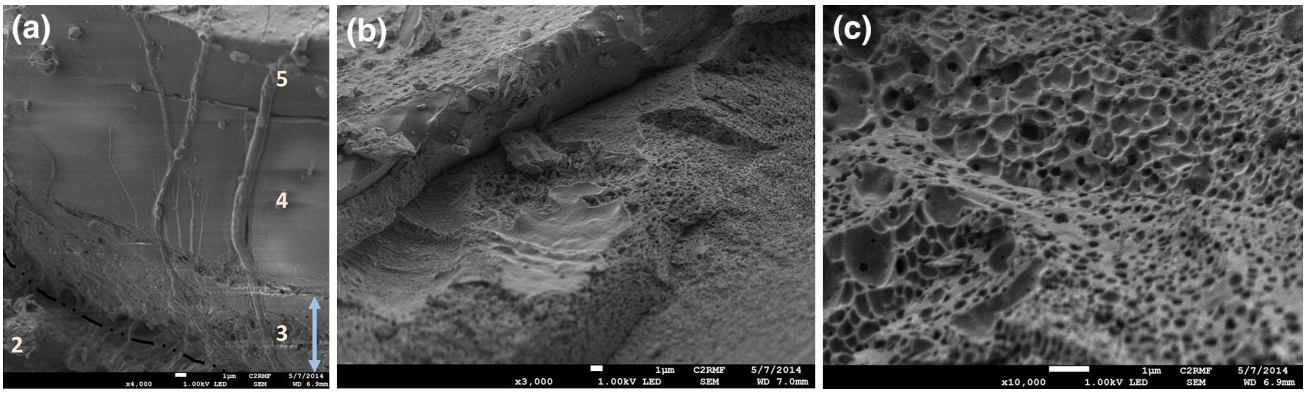

Fig. 4 Varnish sample from Louis Crignier, Jeanne d'Arc en prison. FEG-SEM images at 1 kV; *scale bar* 1 µm. **a** Edge of the sample, the presence of porosity in the blanched layer 3; **b** Surface of the altered layer 3; **c** Detail of the surface of layer 3

ensure the non-modification of the internal structure of the sample. It has been proved that the embedding in resin can change this structure (resin penetration, polishing). [22] This approach enables to reveal for the first time that the altered layers have an unexpected highly porous (spongious) structure (Fig. 4). There is a high correlation between the localization of the porosity in the stratigraphy of varnish layers and the whitening. Indeed, in our sample, the pores are only present in layer 3 that has become white and opaque (Fig. 4a) but not in layers 4 and 5. A pore size ranging from ca. 100 nm to 1 µm was noticed (Fig. 4b, c). Moreover, no porosity was observed in the unaltered samples.

Mock-up samples prepared by immersing natural varnish (mastic and dammar) and synthetic varnish (Paraloid B72, Laropal A81, Regalrez 1094, MS2A) in ultrapure water at room temperature were studied. Under these conditions, both types of natural varnish have changed but with different alteration kinetics. The blanching of the dammar varnish appears more rapidly. Nevertheless, after 31 days, the blanching is more visible for the mastic than for the dammar varnish. The follow-up of this alteration reveals that the translucent varnish does not become directly white. It highlights a bluish effect in the first days. Photographs of the mastic varnish in visible reflected and transmitted light at T0 and after 1.5, 15, and 31 days are reported in Fig. 5. For the unaltered varnish (T0), the white light is transmitted through the layer. When the layer is light blue (T15), the transmitted light has a low intensity and is rather yellow/orange. However, the light is almost not transmitted by the white layer (T31) which appears more opaque. Some premature cracks are visible due to a poor adhesion between the glass slide and the varnish layer.

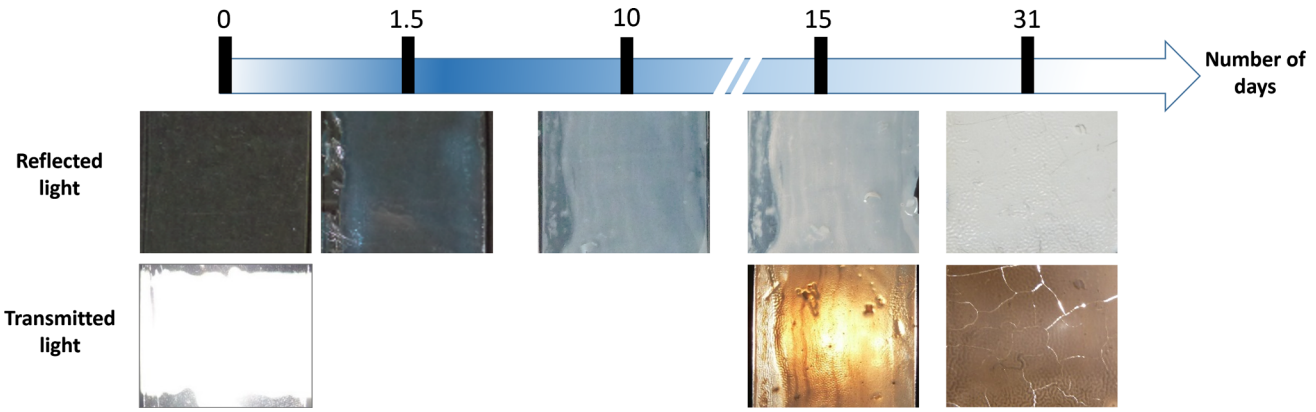

Fig. 5 Photographs taken in reflected (on a *black background*) and in transmitted light at different times of sample evolution

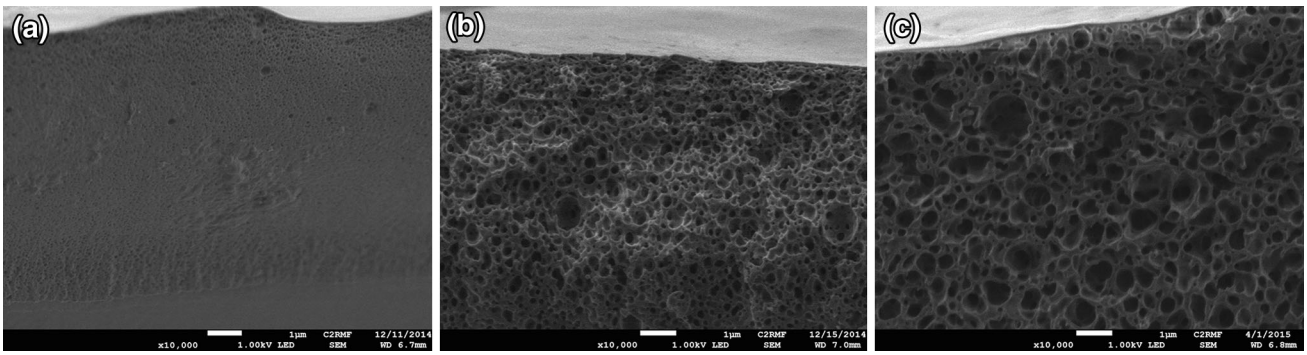

Fig. 6 Mastic varnish samples from mock-ups. FEG-SEM images at the same magnification at 1 kV; *scale bar* 1 µm. **a** $T = 1.5$ days; b) $T = 5.5$ days; **c** $T = 31$ days

Concerning the synthetic varnishes, no visible whitening has been observed under the same alteration conditions, except for the Laropal A81 where a light haze has been detected after 15 days. The synthetic varnishes do not develop any porosity in the conditions of our experiments.

The samples were studied by FEG-SEM to bring to light the presence or absence of porosity. Observations performed at the same magnification on mastic varnish at three steps of the alteration are reported in Fig. 6. A significant increase in the porosity size is observable between T1.5 and T31. A pore size distribution corresponding to these three samples is presented in Fig. 7: T1.5 in black, T5.5 in green, and T31 in red. A pore size of ca. 20 to 300 nm with a maximum in the range 40 to 50 nm has been noticed for the sample T1.5 (blue in reflected light) (Figs. 6a, 7) near the surface. The sample T5.5 (between blue and white in reflected light) has a pore size ranging from ca. 25 nm to 1 µm (Figs. 6b, 7) in almost the full thickness. Finally, the opaque white sample totally altered, T31, is composed of a combination of small and interconnected large pores of ca. 25 nm–2 µm (Figs. 6c, 7). The average porosity size of the sample T5.5 is comparable to the one observed on Louis Crignier's painting (Fig. 4). The protocol used to reproduce the alteration, namely immersing in ultrapure water at room temperature, is therefore valid.

The visualization of these porosities is a major advance for the understanding of the alteration. Indeed, the refractive index difference between the varnish ($n = 1.53$–1.55) and the pores probably filled with air ($n = 1$) leads to a strong light scattering in the layers. The porosities can be assimilated to spherical particles, and the scattering Rayleigh and Mie theories can therefore explain the visual appearance of the altered varnishes. The Rayleigh theory [23, 24] is used for particle sizes much smaller than the wavelength of light (radius of maximum ca. 25 nm). The intensity of the scattered radiation, I, is proportional to λ^{-4}, so that the shorter wavelength (blue) will be 16 times more scattered than the longer wavelength (red). Moreover, as the blue radiations are scattered by particles, only the red radiations will be transmitted. Consequently, for a varnish with pores of mainly 40–50 nm like sample T1.5 (Fig. 6a), blue radiations are more scattered than red ones, and the sample appears blue in reflection and red in transmission. It perfectly fits the observed color in reflected and transmitted light (Fig. 5).

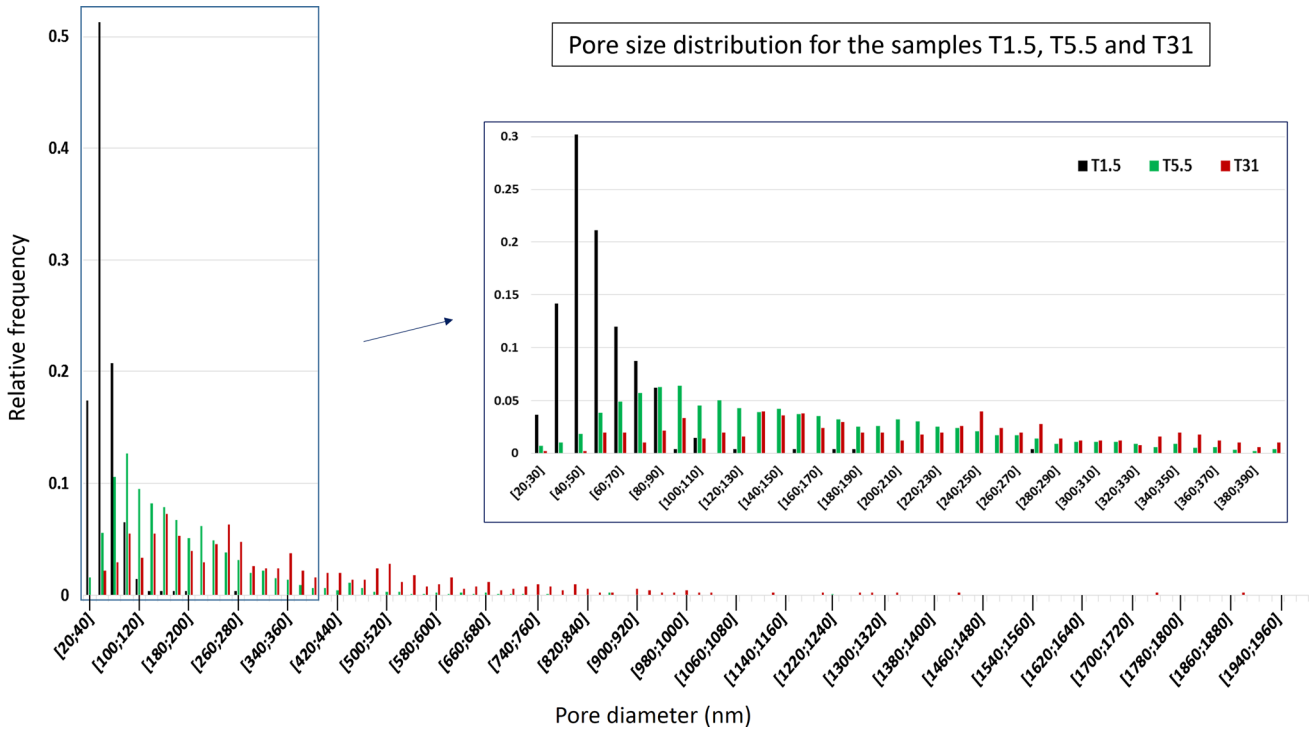

Fig. 7 Pore size distribution for the samples T1.5 (*in black*), T5.5 (*in green*), and T31 (*in red*)

When the particle size is greater than 50 nm, the Mie theory [24, 25] should be used. Contrary to the Rayleigh scattering, the Mie scattering is not wavelength-dependent. It induces a scattering of all wavelengths and therefore a white color. In sample T31 (Fig. 6c), the pores are large and in high concentration. It induces an important scattering, and the light is almost not transmitted through the layers. As the size of the pores increases with the immersing time, the sample will follow Rayleigh theory at the beginning of the pore formation until a particle size of ca. 50 nm (blue color) and then Mie theory (white color). However, there is an important size distribution, and pores of more or less than 50 nm can coexist during the growing process, explaining why some samples appear light blue (both Rayleigh and Mie scatterings).

When the pore size increases, the porosity concentration becomes relatively high, and it induces an interconnection of the pores. Consequently, the percentage of solid matter will be too low to ensure the layer cohesion, leading to a possible cleavage between the varnish and the paint layers. This case has already been observed on the painting of Louis Crignier in the much altered areas. The results obtained for the varnish are summarized in Fig. 8.

3.2 Blanching of paint layers

About 40 paint microsamples were studied to ensure a significant sampling (Table 1). They were taken in altered and unaltered areas mainly from green, brown, and dark colors, except for *L'Aurore*, a particularly altered painting, where orange, purplish, and flesh colors were, for instance, sampled [26] (Table 1).

All samples were studied by FEG-SEM. The results obtained from two samples originating from the painting *Portrait de Louise-Marie de France, dite Madame Louise*, workshop of Jean-Marc Nattier (1685–1766) are presented in Fig. 9. As blanching does not appear homogeneous, altered, less altered, and unaltered areas can coexist within a same color range. The comparison of an altered sample (sample 1—Fig. 9b) with a partially altered sample (sample 2—Fig. 9c) enables to identified the marker of this alteration. The presence of porosity has been observed in the altered sample (Fig. 9d) but not in the unaltered areas of the second sample (Fig. 9e). Due to the presence of pigments, the internal structure of a paint layer differs from that of a varnish layer. Pigment particles impose some constraints to the formation of pores which are less spherical. In all samples, a porosity range from about 100 nm to 2 µm was noticed.

For the mock-ups, it can be observed that the nature of the pigments has an influence on the appearance of the alteration. Indeed, only mock-ups prepared with green earth and raw umber have changed (Fig. 1). No significant difference was detected on azurite and ivory black samples. These results are in agreement with the observations done on ancient paintings during this study and described in

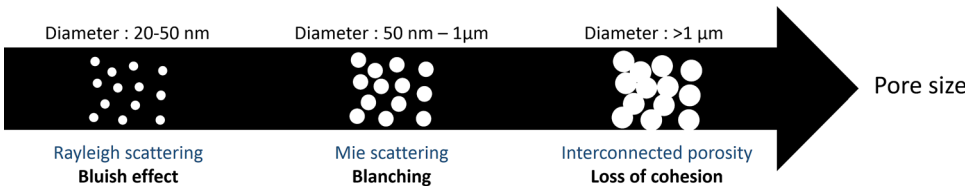

Fig. 8 Correspondence between the visual appearance of the layer, the pore size, and the involved optical phenomenon

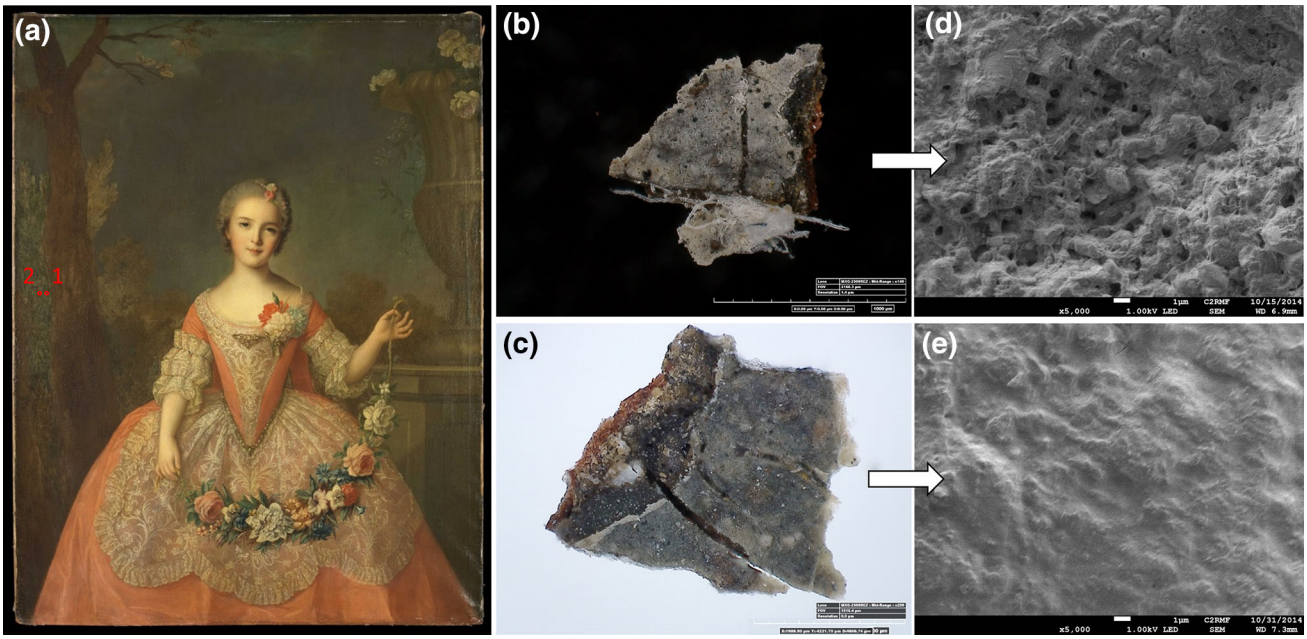

Fig. 9 **a** Photograph in visible light, workshop of Jean-Marc Nattier, Portrait de Louise-Marie de France, dite Madame Louise, 1345 × 1046 mm^2, with the localization of the altered (1) and unaltered (2) samples. ©C2RMF/A; Maigret; **b** Altered sample 1 under visible light, *scale bar* 100 µm; **c** less altered sample 2 under visible light, *scale bar* 500 µm; **d** FEG-SEM image of the altered sample 1 at 1 kV, *scale bar* 1 µm; **e** FEG-SEM image of the unaltered sample at 1 kV. *Scale bar* 1 µm

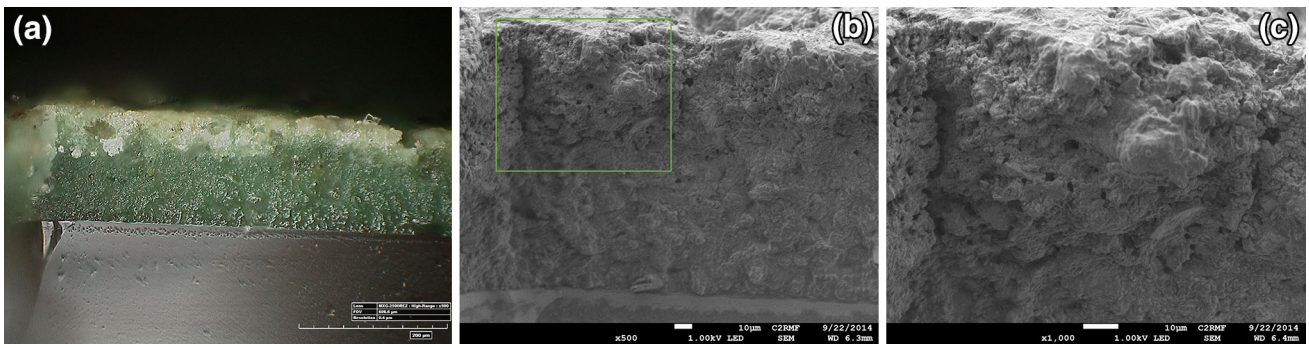

Fig. 10 **a** Edge of the sample B (mock-up) under visible light (HIROX). *Scale bar* 200 µm; **b** FEG-SEM image at 1 kV. *Scale bar* 10 µm. **c** Zoom on the altered part. *Scale bar* 10 µm

previous articles [1, 2, 9, 18]. Additionally, binder preparation has an impact. Samples prepared with recipe 1 are not altered or less altered in a humid environment (climatic chamber) compared to those prepared with recipe 2. The difference between both recipes is the quantity of drier (litharge): 11.1 % in recipe 1 and 4.8 % in recipe 2. Moreover, the addition of chalk as an extender also facilitates the emergence of this alteration.

FEG-SEM images from sample B (green earth, recipe 2, CaCO3, climatic chamber, Fig. 1) are presented in Fig. 10. The alteration of this sample is important but still superficial. The bottom of the stratigraphy is still dark green

(Fig. 10a), and the pigment particles are well agglomerated in the binder (Fig. 10b). At the top, the layer becomes lighter and presents some porosity from 500 nm to 4 µm (Fig. 10b, c). The appearance of the altered layer of this mock-up completely corresponds with the one observed on ancient paintings.

Analyses performed by IRTF and GC–MS on all samples do not reveal so far any significant difference between altered and unaltered samples. The blanching seems, like for the varnish layers, rather due to light scattering. As the pores have a size of more than 50 nm, the blanching can be explained by the Mie scattering of light.

4 Conclusion

The visualization of submicronic to micronic pores (from 40 nm to 2 µm) is a major advance toward the understanding of this alteration of paint and varnish layers. This structural modification was detected thanks to an approach requiring no sample preparation. When using a more traditional method (i.e., embedding in resin and polishing a sample cross section), the resin fills the pores rendering the proper observation impossible. Considering the presence of this porosity in the altered layers, the blanching or the bluish effect observed on ancient paintings and mock-ups can be explained by the Mie or Rayleigh scattering, depending on the pore size. The follow-up of the alteration for varnish layers has revealed that this phenomenon is a dynamic process. It is important to notice that this study has not revealed any microcracks, free fatty acid migration, and pigment alteration, reasons formerly proposed by different authors to explain the blanching.

The phenomenon that contributes to the apparition of this porosity remains so far unclear. However, the influence of different parameters such as quantity of drier (litharge) in the binder, nature of the pigments, and the presence of calcium carbonate was noticed for the blanching of paint layers. The mock-ups revealed also that the supply of humidity and heat is not sufficient to obtain a blanching of the paint layer, the chemical composition of the painting has to be also considered.

The understanding of this phenomenon is a challenging issue, still under investigation at the C2RMF. It could later provide appropriate guidelines for durable conservation treatments that will efficiently and safely attenuate or limit the blanching of paintings.

References

1. M. Wyld, Natl. Gallery Tech. Bull. **4**, 48 (1980)
2. K. Groen, Hamilt. Kerr Inst. Bull. **1**, 48 (1988)
3. M. Debauche, *Les dégats d'eau sur les peintures à l'huile sur toile* (Ecole nationale des Arts visuels de la Cambre (Thesis), 1990)
4. S. Bergeon, P. Curie, *Peinture & dessin: vocabulaire typologique et technique* (Éditions du patrimoine, 2009)
5. J. Plesters, Natl. Gallery Tech. Bull. **4**, 61 (1980)
6. J. Mills, Natl. Gallery Tech. Bull. **4**, 60 (1980)
7. V. Stedman, *Les chancis de vernis* (IFROA, Institut français de restauration des œuvres d'art, Thesis, 1986)
8. C. Bergeaud, J.F. Hulot, A. Roche, La dégradation des peintures sur toile: méthode d'examen des altérations (École nationale du patrimoine, 1997)
9. S. Bergeon, G. Mondorf, S. Delbourgo, J.P. Rioux, Le blanchiment : un cas précis d'étude, In *ICOM-CC, 6th Triennial Meeting*, Ottawa, 21–25 September 1981, Preprints, vol. 4, 81/20/3 (1981)
10. A. Burnstock, M. Caldwell, M. Odlyha, A technical examination of surface deterioration of Stanley Spencer's paintings at Sandham Memorial Chapel, In *ICOM-CC, 10th Triennial Meeting*, Washington, 22–27 August 1993, Preprints (J. Bridgland, ed.), vol. 1, 231 (1993)
11. J. Verhave, A. van Loon, P. Noble, Art Matters Neth Tech. Stud. Art **4**, 103 (2007)
12. A. van Loon, J. Boon, The whitening of oil paints films containing bone black, In *ICOM-CC, 14th triennial Meeting The Hague*, 12–16 September 2005, Preprints (I. Verger, ed.) vol 1, 511 (2005)
13. J. Maroger, *The Secret Formulas and Techiques of the Masters* (Dessain et Tolra, Paris, 1986)
14. T. De Mayerne, Le manuscrit de Turquet de Mayerne: pictoria, sculptoria & quae subalternarum artium (Audin, 1620)
15. M. Cotte, E. Checroun, J. Susini, P. Dumas, P. Tchoreloff, M. Besnard, P. Walter, Talanta **70**, 1136 (2006)
16. M. Cotte, E. Checroun, J. Susini, P. Walter, Appl. Phys. A **89**, 841 (2007)
17. C. Yvel, Le métier retrouvé des maîtres - La peinture à l'huile (Flammarion/Arts et Métiers Graphiques, 1991)
18. S. Lhomme, La problématique des chancis de couche picturale en conservation-restauration (Ecole du Louvre (Thesis), 2014)
19. M. von der Goltz, J.R.G. Proctor, J. Whitten, L. Mayer, G. Myers, A. Hoenigswald, M. Swicklik, in *Conservation of Easel Paintings*, ed. by J. H. Stoner, R. Rushfield (Taylor & Francis, 2013), p. 635
20. J. Mills, R. White, in *Organic Chemistry of Museum Objects* (Taylor & Francis, 2012), p. 95
21. A.N. Assimopoulou, V.P. Papageorgiou, Biomed. Chromatogr. **19**, 285 (2005)
22. C. Gervais, J. Boon, F. Marone, E.B. Ferreira, Appl. Phys. A **111**, 31 (2013)
23. J.W. Strutt, Philos. Mag. Ser. **4**(41), 274 (1871)
24. M. Elias, J. Lafait, La couleur: lumière, vision et matériaux (Belin, 2006)
25. G. Mie, Ann. Phys. **330**, 377 (1908)
26. A. Genty-Vincent, M. Eveno, A. Mohen, C. Toussat, G. Bastian, J. Langlois, M. Menu, Blanching of the superficial paint layers of L'Aurore, a 17th-century French painting. Contribution to the understanding of the alteration and study of conservation treatments, In *ICOM-CC, 17th Triennial Meeting*, Melbourne, 15–19 September 2014, Preprints (J. Bridgland, ed), Poster 1320 (2014)